Check for updates

Synthesis and application of surface-modified NiFe nanoparticles as a new magnetic nano adsorbent for the removal of nickel ions from aqueous solution

Yan Liu and Xiaoyi Shen

ABSTRACT

Surface-modified magnetic $Ni_{2.33}Fe$ alloy nanoparticles were prepared using a hydrothermal method. Thermogravimetric analysis (TG) and Fourier transform infrared spectroscopy (FTIR) tests demonstrated that the surface was successfully modified by sodium citrate. The surface-modified particles can be used for removing nickel ions from aqueous solution. The adsorption kinetics studies were performed and the pseudo-second-order kinetic model successfully described the kinetic data. The diffusion model indicated the adsorption was regulated by both surface and intraparticle diffusion processes. The Freundlich and Langmuir adsorption models were adopted for the mathematical description of adsorption equilibrium, and it was found that the experimental data fitted very well to the Freundlich model.

Key words | adsorption, Freundlich adsorption model, kinetics, magnetic alloy particles, nickel ion

Yan Liu (corresponding author)
Xiaoyi Shen
School of Metallurgy,
Northeastern University,
Shenyang 110819,
China
E-mail: *liuy@smm.neu.edu.cn*

INTRODUCTION

Heavy metal ions are widely produced in many industries such as galvanization, metallurgy, leather making, chemical industry and printing dyeing, etc. Discharge of wastewater containing heavy metal ions into the water system has caused serious environmental influence. Through drinking and crop irrigation, the polluted water has led to a risk to public health (Peng *et al.* 2004). Thus, effectively and thoroughly removing heavy metal ions from the water system is an important task with great challenges.

During the past decades, many methods have been developed to remove hazardous pollutants from wastewaters, such as coagulation/flocculation (Ahammed *et al.* 2014), chemical precipitation (Zhu *et al.* 2007), membrane filtration (Zheng *et al.* 2013), catalytic and photocatalytic oxidation (Copper & Burch 1999; Larachi *et al.* 2001), chlorination (Sinkkonen *et al.* 1997), reverse osmosis (Arzuada *et al.* 2008) and adsorption (Anbia & Lashgari 2009). Among these techniques, adsorption has attracted great interest and has become to the most common method for heavy metal removal because it is simple and cost-effective.

The traditional adsorbents, such as activated carbon (Guo *et al.* 2010), chitosan (Borsagli *et al.* 2015), zeolites (Nezamzadeh-Ejhieh & Kabiri-Samani 2013), and clays (Kaur *et al.* 2015), suffered from low efficiency. Nowadays, nanomaterials have emerged as a novel probe because of their excellent adsorption ability resulting from their small size and large surface area (Hua *et al.* 2012). For examples, Afkhami *et al.* (2010) developed 2,4-dinitrophenylhydrazine modified γ-Al_2O_3 for removal of Pb^{2+}, Cd^{2+}, Cr^{3+}, Co^{2+}, Ni^{2+} and Mn^{2+} where the adsorption capacity of Ni^{2+} was 18.18 mg/g; Tarasevich *et al.* (2001) also synthesized modified γ-Al_2O_3, achieving an adsorption capacity of 176.1 mg/g for Ni^{2+}. More nanomaterials, such as amino-functionalized silica nano hollow spheres and silica gel (Najafi *et al.* 2012), nano-calcium titanate (Zhang *et al.* 2011), nano manganese dioxide (Fan *et al.* 2005; Su *et al.* 2010), nanosized titanium oxides (Engates & Shipley 2011), nanosized magnesium oxides (Gao *et al.* 2008), nanosized zinc oxides (Kikuchi *et al.* 2006) and carbon nanotubes (Chen & Wang 2006), have been reported as heavy metal ion adsorbents with high adsorption efficiency recently.

However, another challenge has to be faced. Nanosized adsorbents are hard to recycle, while magnetic adsorbents with the characteristic of easy separation are increasingly being recognized (Ambashta & Sillanpää 2010). The most common studies on magnetic adsorbents focus on ferric oxide (Gupta & Nayak 2012), ferriferous oxide (Yuan *et al.* 2010) and Fe (Boparai *et al.* 2011) because of their satisfactory

doi: 10.2166/wst.2017.453

Downloaded from http://iwaponline.com/wst/article-pdf/76/10/2851/241834/wst076102851.pdf
by guest

capacity for adsorption of toxic matter from aqueous solution (for example, the adsorption of capacities of Ni^{2+} was 23.6 mg/g (Hu *et al.* 2006). Nevertheless, these particles easily lose their magnetism due to oxidization in air or in water.

Magnetic NiFe alloy nanoparticles exhibit improved oxidation resistance. Different to similar NiFe alloy particles that we reported previously (Liu *et al.* 2014), in this study the surface-modified magnetic NiFe alloy nanoparticles can effectively adsorb heavy metal ions, so they were chosen to study the mechanisms of adsorption and to analyse the adsorption isotherms. Because the novel particles can keep their magnetic property longer, they have more potential to be used repeatedly. Moreover, we are expecting to develop a better adsorbent by the combination of the magnetic particles and ordinary adsorbing materials.

EXPERIMENTAL

Preparation of $Ni_{2.33}Fe$ nanoparticles

The NiFe nanoparticles were synthesized using the hydrothermal method (Liu *et al.* 2015). Typically, 3:1 molar ratio of $NiCl_2{\cdot}6H_2O$ to $FeSO_4{\cdot}7H_2O$ and sodium citrate was dissolved into a specific volume of deionized water. 32 mL of 1 M NaOH was added to the solution to adjust the pH to around 12.5. An excess of hydrazine hydrate was dropped into the solution as a reducing agent. The mixture solution was transferred to an autoclave after being stirred well under N_2. The autoclave was sealed and put into a furnace, which was preheated to 120 °C. The autoclave was cooled to room temperature after heating for 19 h. NiFe nanoparticles were separated with a magnetic bar from the solution. The products obtained were cleaned and re-dispersed in deionized water and ethanol several times.

UV-vis spectrophotometry was used to determine the concentrations of nickel ions under the condition of diacetyldioxime as a chromogenic agent.

Another kind of NiFe particle was obtained by the above method by only changing the dosage of sodium citrate. In the paper, the NiFe particle was prepared under the condition of a molar ratio of the total of Ni and Fe salts to sodium citrate of 1:10, the NiFe particle reported before was of a molar ratio of 1:0.2 (Liu *et al.* 2014).

Characterization of the synthesized materials

X-ray diffraction (XRD) patterns were recorded by a Rigaku D/MAX 2500 diffractometer. Scanning electron microscopy (SEM) was performed on a Zeiss Ultra Plus model. Magnetization measurement (VSM) was undertaken using a Lakeshore Model 7407 Vibrating Sample Magnetometer at room temperature. Thermogravimetric analysis (TG) was performed on a TA Instruments SDT Q600. The Fourier transform infrared spectroscopy (FTIR) measurements were performed on a Perkin–Elmer Spectrum 100.

Adsorption experiments

For the equilibrium experiment, 100 mg $Ni_{2.33}Fe$ nanoparticles were added into 30 mL Ni^{2+} solution at a series of known initial concentrations (C_0), where the pH value of the Ni^{2+} solution was controlled at 5.0–5.5. After stirring the samples for 24 h with an agitator, the magnetic particles were separated from the solution using a magnet.

The amount of the adsorbed Ni^{2+} to the magnetic adsorbents was calculated using Equation (1)

$$q_e = \frac{(C_0 - C_e)}{m} \times V \tag{1}$$

For kinetic experiments, zero time was taken as when 200 mg of $Ni_{2.33}Fe$ nanoparticles was added into 200 mL of Ni^{2+} solution with different initial concentrations. The solution was stirred and sampled at appropriate time intervals.

RESULTS AND DISCUSSION

Characterization of adsorbent

Compared with the particles we synthesized previously (Liu *et al.* 2014), the dosage of sodium citrate in the synthesis as a capping agent showed great influence on the composition, morphology and heat stability of NiFe alloy particles.

The compositions of Ni and Fe in the as-synthesized NiFe nanoparticles were determined using the inductively coupled plasma optical emission spectrometry (ICP-OES) method. The ratio of Ni to Fe is 2.33:1, so the particles can be expressed as $Ni_{2.33}Fe$. The other particles we reported before (Liu *et al.* 2014) were $Ni_{3.54}Fe$. This demonstrated that the dosage of sodium citrate had significant impact on the compositions of the bimetallic particles. The basic characterizations for the alloys, including XRD, SEM, transmission electron microscopy (TEM) and magnetic property, are in the Supporting Information (available with the online version of this paper).

To prove sodium citrate modified to the surface of NiFe alloy particles, TG and IR were tested.

Downloaded from http://iwaponline.com/wst/article-pdf/76/10/2851/241834/wst076102851.pdf
by guest

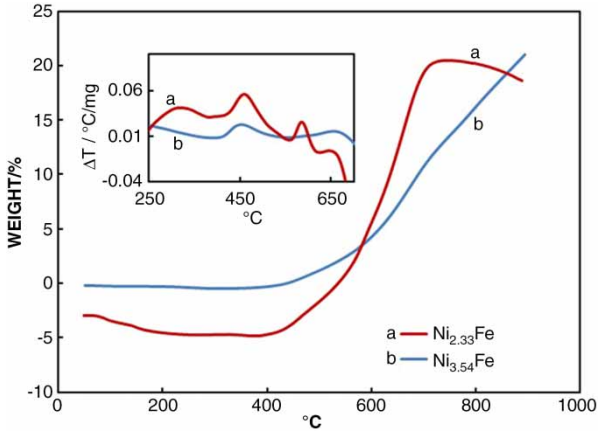

Figure 1 | Thermogravimetric curves for nanoparticles synthesized from different citrate usages: (a) $Ni_{2.33}Fe$, (b) $Ni_{3.54}Fe$.

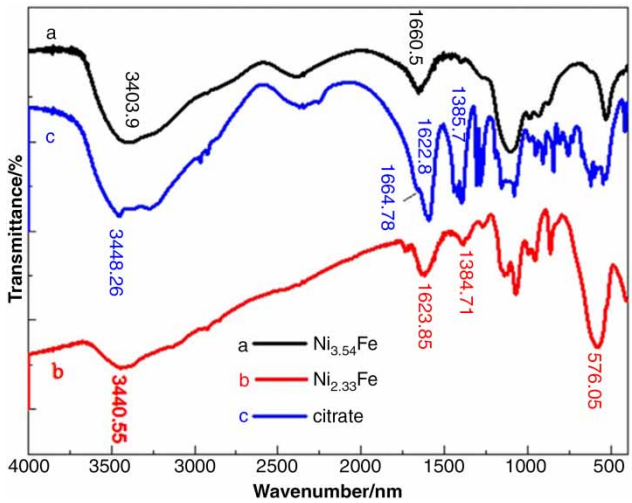

Figure 2 | IR spectra of nano $Ni_{3.54}Fe$, nano $Ni_{2.33}Fe$ and sodium citrate: (a) $Ni_{3.54}Fe$, (b) $Ni_{2.33}Fe$, (c) citrate.

The TG and DTA data for $Ni_{2.33}Fe$ and $Ni_{3.54}Fe$ are shown in Figure 1. For $Ni_{3.54}Fe$, its baseline is flat below 400 °C, explaining that there is no weight loss in the temperature range. The further information deduced is that the surface of the $Ni_{3.54}Fe$ particles does not adsorb volatile molecules, such as water or ethanol. A sharp weight increase started at 400 °C, originating from the oxidation of Fe and Ni at 450 °C and 656 °C (inset curve b) (Liu *et al.* 2014).

An obvious difference for $Ni_{2.33}Fe$ particles is that a weight loss of about 4.7% is observed below 400 °C. The weight loss comes from the volatilization of the water or ethanol bound to the $Ni_{2.33}Fe$ particles. The same as $Ni_{3.54}Fe$ particles, a sharp weight increase started at 400 °C, but the weight increase comes from the oxidation of Fe and Ni at 448 °C and 582 °C. Another difference appeared at 718 °C, with $Ni_{2.33}Fe$ particles exhibiting weight loss while $Ni_{3.54}Fe$ particles showed a weight increase. The weight loss of $Ni_{2.33}Fe$ particles is attributed to the decomposition of citrate bound to the surface of the particles.

Further evidence about the existence of sodium citrate bound to the surface of $Ni_{2.33}Fe$ particles was based on the characteristics of IR spectra (Figure 2). Comparison of the FTIR spectra of nano $Ni_{3.54}Fe$, nano $Ni_{2.33}Fe$ and sodium citrate, it can be obviously seen from Figure 2 that there was a strong stretching vibration peak of C = O at 1,623 cm^{-1} in curve b; the same peak can be found in curve c, but the peak did not appear in curve a. The clear evidence shows that the surface of $Ni_{2.33}Fe$ was bound by sodium citrate, but $Ni_{3.54}Fe$ was not.

The magnetic properties were characterized using a vibrating sample magnetometer at room temperature. The magnetization hysteresis curves of two samples show S-shapes, characteristic of magnetically-soft materials. For $Ni_{2.33}Fe$, the values of the remanence (*Mr*), saturation magnetization (*Ms*) and coercivity (*Hc*) are 2.91 emu·g^{-1}, 75.44 emu·g^{-1} and 45.9 Oe; they are 1.0 emu·g^{-1}, 56.3 emu·g^{-1} and 14 Oe for $Ni_{3.54}Fe$, respectively.

Adsorption of Ni^{2+}

Adsorption kinetics

Lagergren's equation is the most widely used model for the adsorption of solute from a liquid solution. The pseudo-first-order kinetic equation is

$$\log(q_e - q_t) = \log(q_e) - \frac{Kt}{2.303} \tag{2}$$

The pseudo-second-order equation is expressed as follows:

$$\frac{t}{q_t} = \frac{1}{k' q_e^2} + \frac{1}{q_e} t \tag{3}$$

where q_e and q_t (mg/g) are the amounts of Ni^{2+} adsorbed on $Ni_{2.33}Fe$ at equilibrium and at time *t*, respectively. *K* is the kinetic constant of pseudo-first-order adsorption (min^{-1}), and k' is the pseudo-second-order rate constant (g/(mg min)).

If the second order kinetic equation fits the data well, q_e and k' can be determined through the slop and intercept of the plot because of a linear relationship of t/q_e against *t* of Equation (3).

Adsorption dynamics of Ni^{2+} by nanomagnetic particles of $Ni_{2.33}Fe$ were investigated at different initial concentrations of Ni^{2+} and the results are shown in Figure 6. It is clear that the q_t has a rapid increase for contact time within 30 min, and

Downloaded from http://iwaponline.com/wst/article-pdf/76/10/2851/241834/wst076102851.pdf
by guest

sorption equilibration was achieved by 270 min, followed by a constant adsorption rate with further shaking time.

The values of $\log(q_e - q_t)$ were calculated from the kinetic data of Figure 3 and plotted versus t of Equation (2). The adsorption parameters and the plots from pseudo-first-order kinetic model are presented in Table 2.

It can be found the corresponding regression coefficient (R^2) based on the pseudo-first-order model is low ($R^2 < 0.85$), and the theoretical q_e values predicted by this model are very different to the experimental q_e values at different initial concentrations of Ni^{2+}.

Figure 4 shows the plots of the pseudo-second-order kinetic model for adsorption on magnetic nano-$Ni_{2.33}Fe$, where t/q_e is plotted against t. And adsorption kinetic parameters based on the pseudo-second-order equation (Equation (3)) are presented in Table 1. The theoretical q_e values predicted by this model agree very closely to the experimental q_e values at different initial adsorbate concentrations. Further, a good linearity with R^2 above 0.999 also indicates the adsorption kinetics follows the pseudo-second-order model.

Adsorption rate-controlling mechanism

The results obtained using the pseudo-second-order model are not enough to predict the diffusion mechanism (Akar *et al.* 2008). Therefore, the intraparticle diffusion model is investigated to analyze the adsorption kinetic data.

Intraparticle diffusion model based on the theory proposed by Weber and Morris was tested as

$$q_t = k_d t^{1/2} + C \tag{4}$$

where K_d (mg/g $min^{1/2}$) is the intraparticle diffusion rate constant, and C (mg/g) is a constant related to the thickness of the boundary layer. If the plot of q_t versus $t^{1/2}$ gives a straight line and the straight line passes through the origin, then the sorption process is controlled by intraparticle diffusion only. However, if the data exhibit multi-linear plots, then the sorption process is controlled by two or more steps. The first, sharper portion is the external surface adsorption or instantaneous adsorption stage. The second portion is the gradual adsorption stage, where the intraparticle diffusion is rate limited.

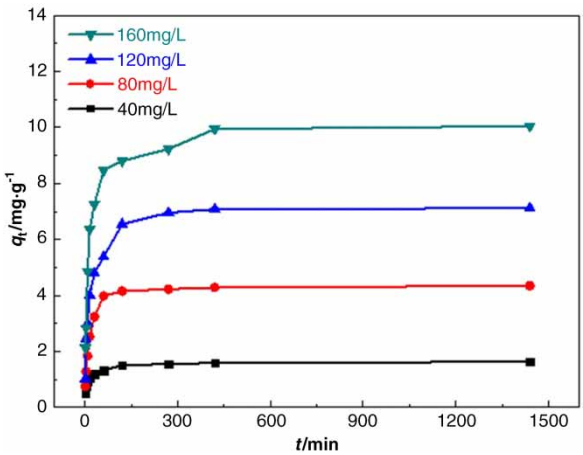

Figure 3 | Ni^{2+} adsorption kinetics on magnetic $Ni_{2.33}Fe$ nanoparticles at 20 °C; initial Ni^{2+} concentrations: (a) 40 mg/l, (b) 80 mg/l, (c) 120 mg/l, (d) 160 mg/l.

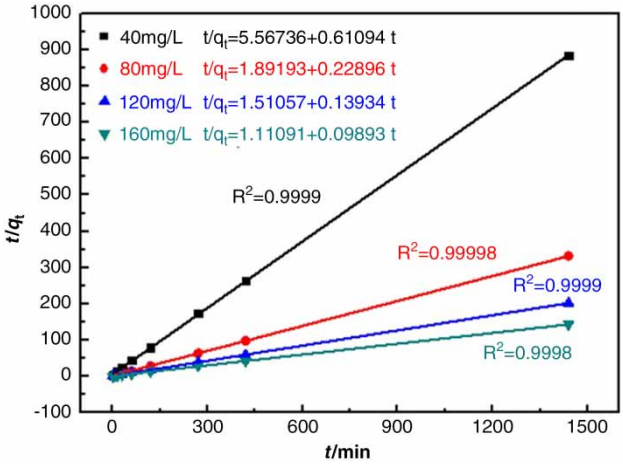

Figure 4 | Plot of pseudo-second-order model at different concentrations of Ni^{2+} for $Ni_{2.33}Fe$ as adsorbent.

The diffusion model plots shown in Figure 5 are related by two straight lines during the adsorption process, indicating the adsorption was regulated by both the surface and intraparticle diffusion processes. The first linear portion of the plot indicates the boundary layer effect, i.e. surface adsorption while the second linear portion is due to the intraparticle diffusion. Moreover, no line passes through the original point. All these facts prove that intraparticle diffusion is not the only controlling factor. The slope of the second linear portion of the plot has been defined as a rate parameter (k_d), which characterizes the rate of adsorption in the region where pore diffusion is rate limiting. Thus, all these suggest that in the adsorption of Ni^{2+} over the nano $Ni_{2.33}Fe$ was controlled by external mass transfer followed by intraparticle diffusion mass transfer.

The values of K_{id} and C_i are listed in Table 2. It can be found that K_{i1} is larger than K_{i2}, while C_1 is smaller than C_2, demonstrating that the global adsorption process is controlled by intraparticle diffusion.

Adsorption isotherms

The Langmuir equation can be expressed as

$$\frac{C_e}{q_e} = \frac{C_e}{q_m} + \frac{1}{q_m K_L} \tag{5}$$

Downloaded from http://iwaponline.com/wst/article-pdf/76/10/2851/241834/wst076102851.pdf
by guest

Table 1 | Determined kinetic model constants for the adsorption of Ni^{2+} on $Ni_{2.33}Fe$ at different initial concentrations

		Pseudo-first-order			Pseudo-second-order		
C_0 (mg/L)	q_e (mg/g) exp.	K (/min)	R^2	q_e*	K' (g/mg min)	R^2	q_e*
40	1.6295	0.00323	0.8245	0.468	0.06704	0.9998	1.6368
80	4.343	0.00312	0.6528	1.096	0.02771	0.9999	4.3676
120	7.117	0.00315	0.6584	2.135	0.01285	0.9999	7.1768
160	10.044	0.00314	0.7589	3.200	0.00881	0.9999	10.1082

Note: q_e*, (mg/g), calculated from pseudo-first-order model and pseudo-second-order model.

Table 2 | The intraparticle diffusion parameters for Ni^{2+} adsorption onto $Ni_{2.33}Fe$

Initial concentration (mg/L)	K_{i1} (mg/g min$^{1/2}$)	C_1	R^2	K_{i2}	C_2	R^2
40	0.113	0.533	0.922	0.0044	1.474	0.879
80	0.480	0.459	0.981	0.010	4.006	0.724
160	0.963	1.68	0.931	0.051	8.336	0.767

where q_e is the equilibrium adsorption capacity of pollutants on the adsorbent (mg/g), C_e the equilibrium pollutant concentration in solution (mg/L), q_m is the maximum capacity of the adsorbent (mg/g), and K_L is the Langmuir adsorption constant (L/mg).

The linear form of the Freundlich equation, which is an empirical equation used to describe heterogeneous adsorption systems, can be represented as follows:

$$\ln q_e = \ln K_F + \frac{1}{n}\ln C_e \quad (6)$$

where q_e and C_e are defined as above, K_F is the Freundlich constant (L/mg), and n is the heterogeneity factor.

The values of q_m and K_L were determined from the slope and intercept of the linear plots of C_e/q_e versus C_e, and values of K_F and 1/n were determined from the slope and intercept of the linear plot of ln q_e versus lnC_e.

The equilibrium adsorption capacities of Ni^{2+} are fitted by Langmuir and Freundlich isotherm equations (Equations (5) and (6)), and the results of the data fitting are shown in Figure 6. In the Langmuir model, the regression coefficient, $R^2 =$ 0.8025, is low, and the slope of the line is a negative value. It will provide an unreasonable negative value of q_m. This implies that the Langmuir model could not represent the data reasonably well. The Langmuir describes monolayer adsorption, and this means monolayer adsorption is not suitable for representing the adsorbing of Ni^{2+} over $Ni_{2.33}Fe$.

The regression coefficient, R^2, is 0.9923 based on fitting the data on the Freundlich model. It obviously fits better to the Freundlich equation than to the Langmuir equation. Thus, the adsorption of Ni^{2+} on $Ni_{2.33}Fe$ obeyed the Freundlich adsorption isotherm. The values of K_F and $1/n$ were determined from the slope and intercept of the linear plot of ln q_e versus lnC_e, and are 0.0177 and

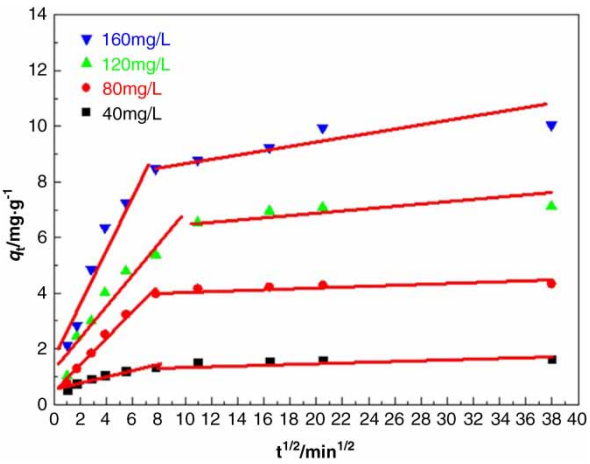

Figure 5 | Plot of Weber-Morris intraparticle diffusion model at different concentrations of Ni^{2+}.

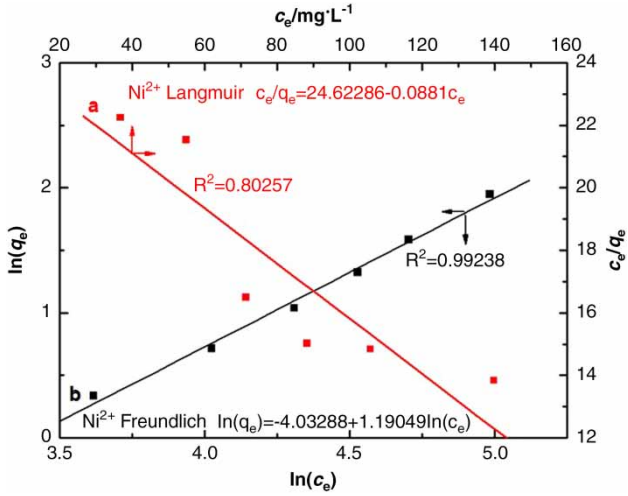

Figure 6 | Adsorption isotherms of Ni^{2+} onto nano-$Ni_{2.33}Fe$: (a) Langmuir, (b) Freundlich.

Downloaded from http://iwaponline.com/wst/article-pdf/76/10/2851/241834/wst076102851.pdf
by guest

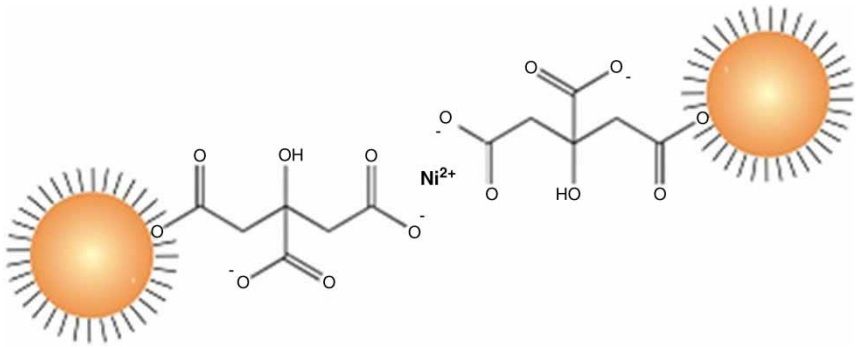

Figure 7 | Model of the surface-modified particles and the adsorption.

1.1905, respectively. The value of $1/n$ between 1 and 2 indicates that Ni^{2+} can be adsorbed by the magnetic $Ni_{2.33}Fe$. The Freundlich model, as an empirical model, is particularly suitable to describe the interaction of multi-layer ions and chemical adsorption.

Based on all that has been discussed above, the models of the surface-modified NiFe nanoparticles in the water and the adsorption for Ni^{2+} can be deduced to be as in Figure 7. Citrates are densely arranged on the surface of the basic unit of NiFe particles by combination with the O^{2-} in one of three carboxylate radicals due to the excessive dosage of sodium citrate during the preparation process. Hence, the existence of sodium citrate in the NiFe magnetic particles can be detected from IR and TG. Further, the wires seen in SEM are grown by the O^{2-} in the second carboxylate radical attached to another NiFe particle. For the adsorption, the chelation between Ni^{2+} and the carboxylate must be generated during the adsorbing process. There are two carboxylates in the sodium citrate to chelate Ni^{2+}, illustrating that the adsorption is via the multisite adsorption Freundlich model, the same as the experimental results. Some analogous results (Zhong *et al.* 2013; Li *et al.* 2015) have been obtained on the effects of sodium citrate on the adsorption. Results from Zhong *et al.* showed that the carboxyl content gave a great enhancement in the adsorption properties of modified activated carbon for copper. Hence, it can be sure that sodium citrate plays a key role in the adsorbing ability of NiFe particles.

CONCLUSIONS

The NiFe bimetallic alloy particles were successfully modified by sodium citrate. The surface-modified magnetic NiFe alloy nanoparticles exhibited the ability to adsorb nickel ions. By comparing the pseudo-first and pseudo-second-order kinetic models, it was found that the pseudo-second-order kinetic model successfully described the kinetic data. The Freundlich and Langmuir adsorption models were adopted to describe the adsorption isotherms, and it was found that the experimental data were best modeled to the Freundlich model.

ACKNOWLEDGEMENTS

The research work was supported by the National Natural Science Foundation of China (NSFC, Grant No. 51574084).

REFERENCES

Afkhami, A., Saber-Tehrani, M. & Bagheri, H. 2010 Simultaneous removal of heavy metal ions in wastewater samples using nano-alumina modified with 2,4- dinitrophenylhydrazine. *Journal of Hazardous Materials* **181** (1), 836–844.

Ahammed, S., Ajoy, S., Gajbhiye, V., Suman, G., Manjaiah, K. & Eldho, V. 2014 Simultaneous removal of multiple pesticides from water: effect of organically modified clays as coagulant aid and adsorbent in coagulation-flocculation process. *Environmental Technology* **35** (17–20), 2619–2627.

Akar, T., Anilan, B., Kaynak, Z., Gorgulu, A. & Akar, S. 2008 Batch and dynamic flow biosorption potential of Agaricus bisporus/Thuja orientalis biomass mixture for decolorization of RR45 dye. *Industrial & Engineering Chemistry Research* **47** (23), 9715–9723.

Ambashta, R. & Sillanpää, M. 2010 Water purification using magnetic assistance: a review. *Journal of Hazardous Materials* **180** (1), 38–49.

Anbia, M. & Lashgari, M. 2009 Synthesis of amino-modified ordered mesoporous silica as a new nano sorbent for the removal of chlorophenols from aqueous media. *Chemical Engineering Journal* **150** (2), 555–560.

Arzuada, J., Lopez-Munoz, M. & Aguado, J. 2008 Temperature, pH and concentration effects on retention and transport of organic pollutants across thin-film composite nanofiltration membranes. *Desalination* **221** (1), 253–258.

Downloaded from http://iwaponline.com/wst/article-pdf/76/10/2851/241834/wst076102851.pdf
by guest

Boparai, H., Joseph, M. & O'Carroll, D. 2011 Kinetics and thermodynamics of cadmium ion removal by adsorption onto nano zerovalent iron particles. *Journal of Hazardous Materials* **186** (1), 458–465.

Borsagli, F., Mansur, A., Chagas, P., Oliveira, L. & Mansura, H. 2015 O-carboxymethyl functionalization of chitosan: complexation and adsorption of Cd (II) and Cr (VI) as heavy metal pollutant ions. *React. Func. Polym.*, **97** 37–47.

Chen, C. & Wang, X. 2006 Adsorption of Ni(II) from aqueous solution using oxidized multi-wall carbon nanotubes, *Industrial & Engineering Chemistry Research* **45** (26), 9144–9149.

Copper, C. & Burch, R. 1999 An investigation of catalytic ozonation for the oxidation of halocarbons in drinking water preparation. *Water Research* **33** (18), 3695–3700.

Engates, K. E. & Shipley, H. J. 2011 Adsorption of Pb, Cd, Cu, Zn, and Ni to titanium dioxide nanoparticles: effect of particle size, solid concentration, and exhaustion. *Environmental Science and Pollution Research* **18** (3), 386–395.

Fan, M., Boonfueng, T., Xu, Y., Axe, L. & Tyson, T. A. 2005 Modeling Pb sorption to microporous amorphous oxides as discrete particles and coatings. *Journal of Colloid and Interface Science* **281** (1), 39–48.

Gao, C. L., Zhang, W. L., Li, H. B., Lang, L. M. & Xu, Z. 2008 Controllable fabrication of mesoporous MgO with various morphologies and their absorption performance for toxic pollutants in water. *Crystal Growth & Design* **8** (10), 3785–3790.

Guo, M. X., Qiu, G. N. & Song, W. P. 2010 Poultry litter-based activated carbon for removing heavy metal ions in water. *Waste Management* **30** (2), 308–315.

Gupta, V. K. & Nayak, A. 2012 Cadmium removal and recovery from aqueous solutions by novel adsorbents prepared from orange peel and Fe_2O_3 nanoparticles. *Chemical Engineering Journal* **180**, 81–90.

Hu, J., Chen, G. H. & Lo, I. M. C. 2006 Selective removal of heavy metals from industrial wastewater using maghemite nanoparticle: performance and mechanisms. *Journal of Environmental Engineering* ASCE **132** (7), 709–715.

Hua, M., Zhang, S., Pan, B., Zhang, W., Lu, L. & Zhang, Q. 2012 Heavy metal removal from water/wastewater by nanosized metal oxides: a review. *Journal of Hazardous Materials* **211–212**, 317–331.

Kaur, M., Singh, M., Mukhopadhyay, S. S., Singh, D. & Gupta, M. 2015 Structural, magnetic and adsorptive properties of clay ferrite nanocomposite and its use for effective removal of Cr (VI) from water. *Journal of Alloys and Compounds* **653**, 202–211.

Kikuchi, Y., Qian, Q. R., Machida, M. & Tatsumoto, H. 2006 Effect of ZnO loading to activated carbon on Pb (II) adsorption from aqueous solution. *Carbon* **44** (2), 195–202.

Larachi, F. F., Ihuta, I. & Belkacemi, K. 2001 Catalytic wet air oxidation with a deactivating catalyst analysis of fixed and sparked three-phase reactors. *Catalysis Today* **64** (3), 309–320.

Li, Y., Bi, H. Y. & Shi, X. Q. 2015 Simultaneous adsorption of heavy metal and organic pollutant onto citrate-modified layered double hydroxides with dodecylbenzenesulfonate. *Environmental Engineering Science* **32** (8), 666–675.

Liu, Y., Shan, S., Yin, J., Luo, J. & Zhong, C. 2014 Characterization of magnetic NiFe nanoparticles with controlled bimetallic composition. *Journal of Alloys and Compounds* **587**, 260–266.

Liu, Y., Liu, K., Zhang, L. & Zhang, Z. 2015 Removal of Rhodamine B from aqueous solution using magnetic NiFe nanoparticles. *Water Science & Technology* **72** (7), 1243–1249

Najafi, M., Yousefi, Y. & Rafati, A. A. 2012 Synthesis, characterization and adsorption studies of several heavy metal ions on amino-functionalized silica nano hollow sphere and silica gel. *Separation and Purification Technology* **85**, 193–205.

Nezamzadeh-Ejhieh, A. & Kabiri-Samani, M. 2013 Effective removal of Ni(II) from aqueous solutions by modification of nano particles of clinoptilolite with dimethylglyoxime. *Journal of Hazardous Materials* **260**, 339–349.

Peng, S. H., Wang, W. X., Li, X. D. & Yen, Y. F. 2004 Metal partitioning in river sediments measured by sequential extraction and biomimetic approaches. *Chemosphere* **57** (8), 839–851.

Sinkkonen, S., Rantion, T., Paasivitra, J., Peltonen, S., Vattulainen, A. & Lammi, R. 1997 Chlorinated phenolic compound in coniferous needles. Effects of metal and paper industry and incineration. *Chemosphere* **35** (6), 1175–1185.

Su, Q., Pan, B. C., Wan, S. L., Zhang, W. M. & Lv, L. 2010 Use of hydrous manganese dioxide as a potential sorbent for selective removal of lead, cadmium, and zinc ions from water. *Journal of Colloid and Interface Science* **349** (2), 607–612.

Tarasevich, Y. I. & Klimova, G. M. 2001 Complex-forming adsorbents based on kaolinite, aluminium oxide and polyphosphates for the extraction and concentration of heavy metal ions from water solutions. *Appl. Clay Sci.* **19** (1), 95–101.

Yuan, P., Liu, D., Fan, M., Yang, D., Zhu, R., Ge, F., Zhu, J. & He, H. 2010 Removal of hexavalent chromium [Cr(VI)] from aqueous solutions by the diatomite-supported/unsupported magnetite nanoparticles. *Journal of Hazardous Materials* **173** (1), 614–621.

Zhang, D., Zhang, C. & Zhou, P. 2011 Preparation of porous nano-calcium titanate microspheres and its adsorption behavior for heavy metal ion in water. *Journal of Hazardous Materials* **186** (2–3), 971–977.

Zheng, Y., Yao, G., Cheng, Q., Yu, S., Liu, M. & Gao, C. 2013 Positively charged thin-film composite hollow fiber nanofiltration membrane for the removal of cationic dyes through submerged filtration. *Desalination* **328**, 42–50.

Zhong, K. K., Huang, Z. G., Han, X. J. & Zhang, C. M. 2013 Modification of activated carbon using sodium citrate and its effect on the adsorption of copper ions. *Carbon* **60**, 565–565.

Zhu, M., Lee, L., Wang, H. & Wang, Z. 2007 Removal of an anionic dye by adsorption/precipitation processes using alkaline white mud. *Journal of Hazardous Materials* **149** (3), 735–741.

First received 4 May 2017; accepted in revised form 26 July 2017. Available online 11 August 2017

Downloaded from http://iwaponline.com/wst/article-pdf/76/10/2851/241834/wst076102851.pdf
by guest